

Observation and Simulation of Low-frequency Waves on Two Natural Beaches

Satoshi NAKAMURA ¹ and Nicholas DODD ²

Abstract

Field observations of low-frequency wave on natural beaches are carried out. The ratio of the wave height of low-frequency wave near the shoreline to the wind wave height at the offshore has positive correlation with the surf similarity parameter. Using the field data, a validation of a numerical model was made. The model includes basic mechanisms of low-frequency wave generation that low-frequency wave increases with shoaling of wind waves groups, they are released from wave groups due to wave breaking and wind wave period becomes longer due to run-up to the beach. The model results tend to be excessively computed against field data.

Introduction

Low-frequency waves, with wave periods in the order of minutes, appear in the surf zone most noticeably when pronounced wind wave groups exist offshore. Generation of bound or free low-frequency waves can be conclusively explained that the structure of wave group changes. Therefore the low-frequency waves are made everywhere when the wind wave groups change its shape. At the offshore, obtained wave data contain low-frequency waves of all direction from different origin such as bound low-frequency waves grown beneath wind wave group, free low-frequency waves generated near the wave breaking points and from the breakwaters and the shoreline, and low-frequency waves caused by wind wave refraction. In the surf zone, the low-frequency waves, which are mainly generated by wave breaking and become standing waves, occasionally cause rapid nearshore bar migration and berm shape changes by running-up beyond the berm crest.

In this paper, field observations are presented. The simultaneous data of offshore and nearshore low-frequency waves are obtained. A numerical model which includes mechanisms of low-frequency wave generation is used to simulate the observed dynamics.

¹Marine Environment Division, Port and Harbour Research Institute, 3-1-1 Nagase, Yokosuka 239-0826, Japan

²Coastal Group, HR Wallingford, Howbery Park, Wallingford, OX10 8BA, UK.

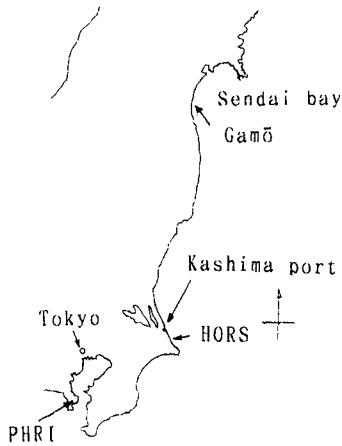


Figure 1: Map of observation sites

Field observation

Study sites

Field studies of low-frequency waves and wave groups have been carried out at two sites of the east coast of Japan (see fig.1).

One field observation has been carried out at a seashore site near Gamō tidal lagoon in the Sendai bay on the Pacific coast since 1997 for the study of wave run-up with the low-frequency waves on a berm and of offshore wave groups. In this observation, wave data were collected continuously with sampling 0.5s intervals using only 2 wave gages at the offshore and near the shoreline. Figure 2 shows the beach profile at Gamō and location of the wave gages. The offshore wave gage, which is set on the sea bottom at 4km offshore from the shoreline and 20m depth, measures the sea surface elevation using ultra-sonic wave. The nearshore ultra-sonic wave gage is attached in the air on a scaffold at the shoreline. A highly-sensitive CCD camera and video recorder, which is set on the berm, is used to record the wave run-up and over-topping events beyond the berm crest. During observation period, an over-topping event does not record unfortunately. We do not use video data in this paper.

Another field observation was carried out at Hazaki Oceanographical Research Station (HORS) in 1989 (see Nakamura and Katoh, 1992) for the study of the propagation of incident wave groups and the low-frequency nearshore

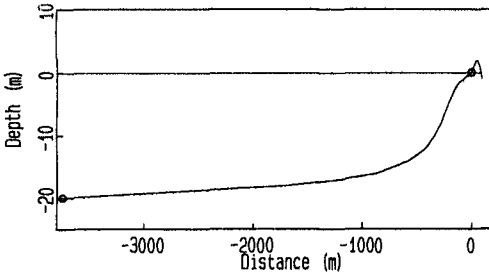


Figure 2: Beach topography of Gamō beach

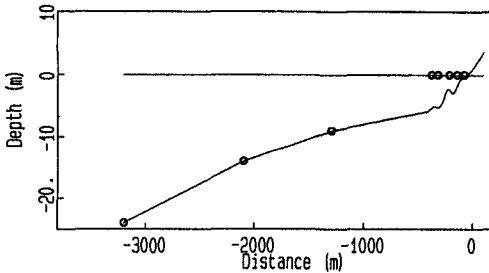


Figure 3: Beach topography of HORS

wave motion in the storm condition. Figure 3 shows the beach profile at HORS and location of the wave gages. This data set contains simultaneous recordings of 10 wave gages from the shoreline to 3.2km offshore during a storm.

Data analysis

A set of wave record, which length is approximately 2 hours, separated in the frequency band upper 0.04Hz and the low-frequency band using FFT method. Significant wind wave heights, H_S , and periods, T_S , are calculated from the higher band wave record using zero-up-cross method. Significant low-frequency wave heights, H_L , and periods, T_L , are calculated same way. For the numerical model input, the wave energy time series is calculated from the wave envelope

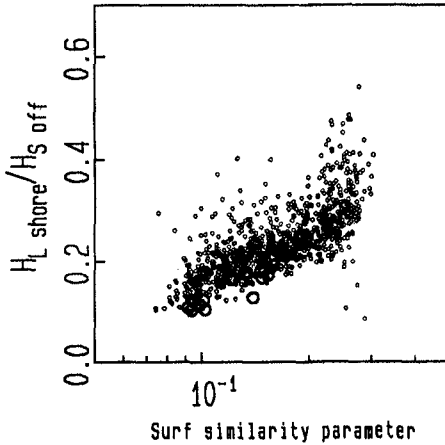


Figure 4: Ratio of the low-frequency wave height in the surf zone to the significant wave height in the offshore vs. surf similarity parameter

using Hilbert transform (see Hudspeth and Medina, 1988) of the wind wave record is used.

Figure 4 shows the ratio of low-frequency wave height near the shoreline, H_{Lshore} , to offshore wind wave height, H_{Soff} , against the surf similarity parameter, $\tan \beta_b / \sqrt{H_{Soff} / L_{Soff}}$, where $L_{Soff} = 1.56 * T_{Soff}^2$ is offshore wave length and $\tan \beta_b$ is the slope of the surf zone in case of Gamō $\tan \beta_b = 1/70$ and in case of HORS $\tan \beta_b = 1/60$. In figure 4, small circles indicate the data obtained at Gamō and large circles at HORS. The ratio of H_{Lshore} / H_{Soff} has positive correlation with the surf similarity parameter. In both cases, the plots seem to be scattered on a line. This fact suggests that height of low-frequency waves in the surf zone becomes large not only as height of offshore wave becomes large but on condition that beach profile and waves fill some requirements.

Figure 5 shows the ratio of low-frequency wave height at the offshore, H_{Loff} , to offshore wave height, H_{Soff} , against the surf similarity parameter. There are two groups of plots in figure 5. One is the ratio of H_{Loff} / H_{Soff} has positive correlation with the surf similarity parameter. Another group is the ratio has no correlation with the surf similarity parameter. The feature of this group is that it appear in Gamō data at the calm condition several days after the storm and it does not appear in HORS data. According to the NOWPHAS

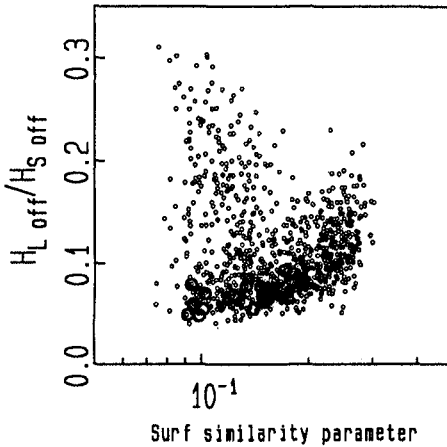


Figure 5: Ratio of the low-frequency wave height to the significant wave height in the offshore vs. surf similarity parameter

data PHRI (1996), at Sendai New Port where is nearest observation point of Gamō, the relative frequency of calm condition ($H_s \leq 0.5m$) is 24.5% and the distribution of incident wave direction is narrow (main direction is SE) and at Kashima Port where is nearest point of HORS, the relative frequency of calm condition is 2.5% and the distribution of incident wave direction is wide (main direction is E). Comparing Gamō with HORS, as Gamō beach is located at the inner part of the bay, heights of significant wind wave quickly decrease after storm due to an effect of interception of Sendai bay. I suppose that trapped small amplitude low-frequency waves in Sendai bay are observed at offshore Gamō beach.

Numerical model

Low-frequency wave model

The numerical model of low-frequency waves uses an upwind, Godunov-type finite volume method to solve the equations. This method alleviates the problem of tracking multiple shorelines, which can occur over barred beaches (see Dodd, 1998; Nakamura and Dodd, 1997). The numerical equations used in the model are the one-dimensional depth-integrated and time-averaged non-linear shallow water equations of mass (eq.1) and momentum (eq.2), in which the

radiation stress gradient is included as a forcing term, and the energy balance of fluctuating motion equation (eq.3) (see e.g. Roelvink, 1993; Zou and Dodd, 1994) includes the interaction of wind wave energy and low-frequency waves.

$$\frac{\partial D}{\partial t} + \frac{\partial(DU)}{\partial x} = 0, \quad (1)$$

$$\frac{\partial(DU)}{\partial t} + \frac{\partial}{\partial x} \left(DU^2 + \frac{1}{2}gD^2 \right) = gD \frac{\partial h}{\partial x} - \frac{\partial}{\partial x} \left(\frac{S_{11}}{\rho} \right) - \tau_b, \quad (2)$$

$$\frac{\partial E}{\partial t} + \frac{\partial}{\partial x} [(c_g + U)E] + \frac{\partial}{\partial x} (US_{11}) = -\mathcal{D}, \quad (3)$$

where D is the total mean water depth, U is the mean velocity, h is the still water depth, τ_b is a bottom friction term, \mathcal{D} is a dissipation term,

$$E = \frac{\rho g}{8} H^2, \quad (4)$$

$$c_g = \frac{1}{2} \frac{\omega}{k} \left(1 + \frac{2kD}{\sinh 2kD} \right), \quad (5)$$

and

$$S_{11} = E \left(2 \frac{c_g}{c} - \frac{1}{2} \right). \quad (6)$$

The interaction terms appear effective close to the shoreline where wave speed and water velocity are nearly equal. To calculate low-frequency waves generation nearshore zone, we use here the 1D model as that the wind wave was being incident on the coastline at the normal angle is supposed for reason that both of near HORS and Gamō beach topography have little change into alongshore direction. To simulate trapped low-frequency wave by alongshore topography such as edge waves, of course, the 2D model has to be used.

Simulations

In this model, the radiation stress gradient works as a forcing term. So, the distribution of the radiation stress seriously affects on the model results. As this model calculate radiation stress using a simple function of wave height (eqs.4-6), we compare the wave height distribution between the field data and the model result. Figure 6 is a comparison of the distribution of mean wind wave height in storm condition ($H_s = 2.4m$, $T_s = 11.8s$) at HORS. Solid line is a model result that is calculated from each steps of the distribution of wave energy simulated by giving a time series of wind wave energy at the offshore boundary. Roelvink's wave dissipation model ($\gamma = 0.65$ and as following Roelvink $\alpha = 1.0, n = 10$) is used in this model results. Circles indicate the field data. The model results of nearshore mean wave height has a good

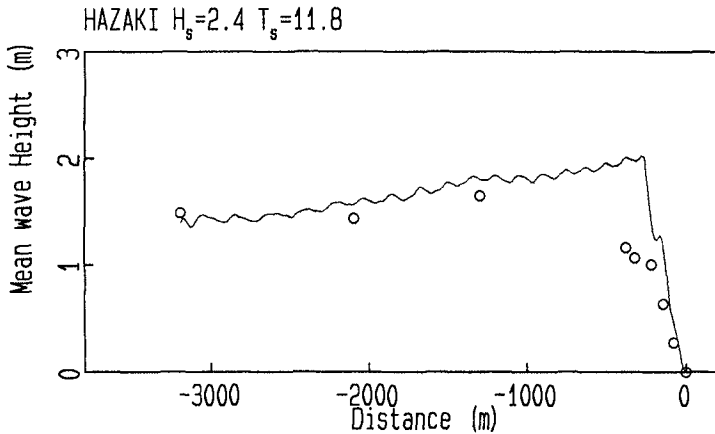


Figure 6: Comparison of mean wave height distribution between field data and model results

agreement with field data but the results of mean wave height near the wave breaking point is over estimated.

Figure 7 shows a comparison of the distribution of low-frequency wave height in same wave condition of fig.6. Bold solid line is a model results. Thin solid line is a model result of mean water level (no comparison with field data). Circles are field data. In model result, low-frequency wave height is calculated excessively. The distance between the field data of low-frequency wave height near the shoreline and the model result of that can be reduced using a large bottom friction coefficient at this region. We do not use such adjustment because it is not essential. At the shoreline (0m), low-frequency wave height in field is not calculated because run-up waves come rarely at this point.

Comparisons

Comparisons of low-frequency wave height between the field data and the model results are done with chose 13 data sets, which are embraced in the group that the ratio of H_{Loff}/H_{Soff} has positive correlation with the surf similarity parameter, in Gamō data sets and 15 data sets in HORS data sets.

Figure 8 shows a comparison of low-frequency wave heights near the shore-

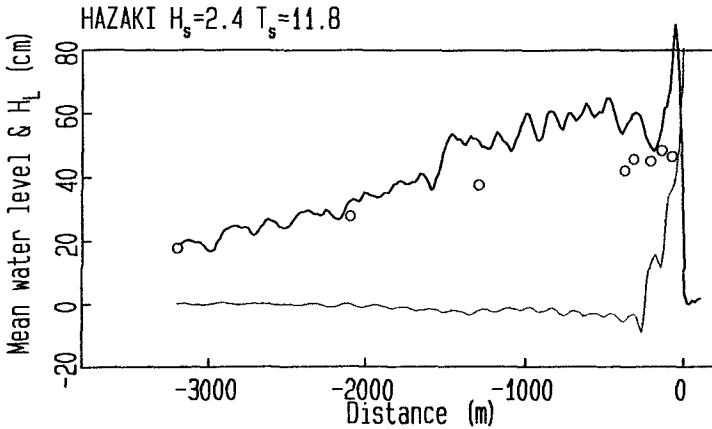


Figure 7: Comparison of low-frequency wave height distribution between field data and model results

line between field data and model results. Small boxes indicate the Gamō data and large boxes the HORS data. The model results become excessive estimation of wave height in proportion that low-frequency wave height in field becomes large. This tendency is explained as the model feature at fig.7.

Figure 9 shows a comparison of low-frequency wave heights in the offshore between field data and model results. Small boxes indicate the Gamō data and large boxes the HORS data. There are three under-estimated results. Except three data, the model results are well computed.

Conclusions

During the observation period at Gamō, a few simultaneous observation records using offshore and nearshore wave gages were gotten. Conspicuous run-up events at Gamō as water invade a lagoon beyond the crest of sand dune aren't observed by video records.

At offshore Gamō beach, the small amplitude of low-frequency waves are observed in calm condition until several days after storms. Comparing Gamō with HORS, as Gamō beach is located at the inner part of the bay, heights of significant wind wave quickly decrease after storm due to an effect of interception of Sendai bay. There seems to be trapped small amplitude low-frequency

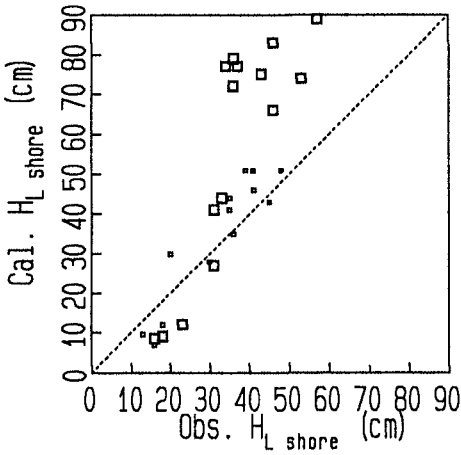


Figure 8: Comparison of low-frequency wave heights near the shoreline between field data and model results

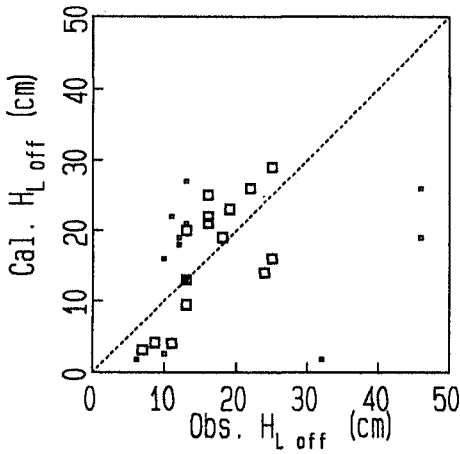


Figure 9: Comparison of low-frequency wave heights in the offshore between field data and model results

waves in Sendai bay.

The computation result of the low-frequency wave tends to be excessively computed. This cause is to compute the energy of the wind wave excessively. To do the better simulation, the wind wave energy dissipation and the bottom friction of the low-frequency wave must be well computed. The way to the better simulation seems to be essential difference that wind wave breaking on the surface low-frequency motion, the radiation stress in breaking waves and sediment moving by low-frequency current.

References

- N. Dodd. A numerical model of wave run-up, overtopping and regeneration. *J. Water. Port Coast. Ocean Eng.*, 1998. To appear.
- R. T. Hudspeth and J. R. Medina. Wave group analysis by the Hilbert transform. In *Proc. 21st Int. Conf. Coastal Eng.*, pages 884–898, Malaga, 1988. A.S.C.E.
- S. Nakamura and N. Dodd. A numerical model of low-frequency wave motion on a beach and over reefs. In *Proc. of Waves'97*, 3rd Int. Symp. On Ocean Wave Measurement and Analysis, 1997. A.S.C.E.
- S. Nakamura and K. Katoh. Generation of infragravity waves in breaking process of wave groups. In *Proc. 23rd Int. Conf. Coastal Eng.*, pages 990–1003, Venice, 1992. A.S.C.E.
- PHRI. Nowphas 1997-1994. Technical report, Port and Harbour Research Institute, MOT, 1996.
- J. A. Roelvink. *Surf beat and its effect on cross-shore profiles*. PhD thesis, Delft University of Technology, 1993.
- Z. Zou and N. Dodd. A nonlinear surf beat model. In *Proc. 24th Int. Conf. Coastal Eng.*, pages 1961–1974, Kobe, 1994. A.S.C.E.